Asian Journal of Chemistry; Vol. 38, No. 7 (2026), 1751-1758
ASIAN JOURNAL OF CHEMISTRY
https://doi.org/10.14233/ajchem.2026.36088

Synthesis of Novel Pyrimido[1,2-*c*]quinazolin-4-one and Triazolo[4,3-*c*]quinazoline Derivatives: Anticancer Activity and Docking Interactions

RAMU PERUMANDLA[1], SAIRAM GUMMULA[1], SHYLAJA KOTTE[2] and SAILU BETALA[1,*]

[1]Department of Chemistry, Telangana University, Dichpally, Nizamabad-503322, India
[2]Department of Chemistry, Mallareddy Engineering College for Women (Autonomous) Dulapally, Secundrabad-500100, India

*Corresponding author: E-mail: bethalasailu@gmail.com

Received: 29 March 2026 *Accepted*: 21 May 2026 *Published online*: 3 July 2026 AJC-22400

A series of novel pyrimido[1,2-*c*]quinazolin-4-one and triazolo[4,3-*c*]quinazoline derivatives were synthesized starting from 2-amino-5-(trifluoromethyl)benzonitrile. The acidic hydrolysis of the nitrile group afforded 2-amino-6-(trifluoromethyl)benzoic acid, which subsequently underwent cyclization in the presence of formic acid to yield the corresponding quinazolinone intermediate. Treatment of this cyclised product with ethyl 2-bromoacetate produced 6-(trifluoromethyl)quinazolin-4-amine. Further condensation of this amine with various substituted ethyl 2-methyl-3-oxobutanoates furnished a series of pyrimido[1,2-*c*]quinazolin-4-one derivatives (**5a-f**). In a parallel synthetic route, 6-(trifluoromethyl)quinazolin-4(3*H*)-one was reacted with phosphorus oxychloride ($POCl_3$) to generate 4-chloro-6-(trifluoromethyl)quinazoline, which further nucleophilic substitution reaction with hydrazine hydrate afforded 4-hydrazinyl-6-(trifluoromethyl)-quinazoline. Finally, cyclocondensation of this intermediate with various substituted aromatic carboxylic acids led to the formation of the target triazolo[4,3-*c*]quinazoline derivatives (**8a-h**). The synthesised pyrimido[1,2-*c*]quinazolin-4-one and triazolo[4,3-*c*]quinazoline derivatives were evaluated for their anticancer potential against four human cancer cell lines, including HeLa (cervical cancer), COLO 205 (colon cancer), HepG2 (liver cancer) and MCF-7 (breast cancer). Biological evaluation revealed that compounds **5a** and **5c** displayed significant anticancer activity compared with the other derivatives. The molecular docking studies were also performed to explore the binding interactions of the most active compounds with the selected biological target and to support the observed experimental results.

Keywords: Trifluoromethyl group, Triazole derivatives, Anticancer activity, Molecular docking interactions.

INTRODUCTION

Heterocyclic compounds constitute an important class of organic molecules containing one or more heteroatoms within their cyclic framework. Among these, quinazolinones represent a significant family of fused heterocycles formed by the fusion of a benzene ring with a 2-pyrimidinone, 4-pyrimidinone or 2,4-pyrimidinedione moiety, resulting in quinazolin-2(1*H*)-one, quinazolin-4(3*H*)-one and quinazolin-2,4-(1*H*,3*H*)-one, respectively [1]. Therefore, the quinazolinone scaffold has also attracted considerable attention owing to its broad spectrum of biological activities including antimalarial [2], antimicrobial [3,4], antitubercular [5], anticonvulsant [6], anticancer [7], antihypertensive [8], antidiabetic [9], anti-inflammatory [10], anticholinesterase [11], cellular phosphorylation inhibition [12], dihydrofolate reductase inhibition [13], kinase inhibition [14], tubulin polymerisation inhibition [15], diuretic [16], antipsychotic [17], dopamine agonistic [18] and anti-HIV activities [19], highlighting their potential as therapeutic agents in cancer treatment.

Similarly, pyrimidine-containing compounds represent another important class of heterocyclic systems with diverse pharmacological properties. Numerous pyrimidine analogues have been reported to exhibit significant biological activities, including anticancer effects [20-24]. Likewise, 1,2,4-triazoles constitute an important group of nitrogen-containing heterocycles that have gained substantial interest in medicinal chemistry due to their wide range of biological properties, especially their promising anticancer potential [25-32].

The combination of multiple biologically active heterocyclic motifs within a single molecular framework has emerged as an effective strategy in the design of new therapeutic agents. In particular, fused pyrimidine- and triazole-containing quinazoline systems have emerged as attractive molecular frameworks in medicinal chemistry, displaying diverse structural features and significant biological potential. However, the

This is an open access journal, and articles are distributed under the terms of the Attribution 4.0 International (CC BY 4.0) License. This license lets others distribute, remix, tweak, and build upon your work, even commercially, as long as they credit the author for the original creation. You must give appropriate credit, provide a link to the license, and indicate if changes were made.

synthesis of such fused heterocyclic systems often requires multistep synthetic procedures, emphasizing the need for efficient approaches to access structurally diverse compounds [27-29].

Among the various structural modifications employed in drug design, the incorporation of fluorine-containing substituents has proven highly beneficial. Trifluoromethyl groups [33-36] can significantly improve lipophilicity, metabolic stability, membrane permeability and oral bioavailability, thereby enhancing the pharmacological properties of heterocyclic molecules. Considering the biological significance of quinazolinone, pyrimidine and triazole scaffolds, together with the favourable effects associated with trifluoromethyl substitution and as a continuation of our ongoing research efforts [35,37], we designed and synthesised a series of novel fluorinated pyrimido[1,2-*c*]quinazolin-4-one derivatives (**5a-f**) and triazolo[4,3-*c*]quinazoline derivatives (**8a-h**). The synthesised compounds were evaluated for their *in vitro* anticancer activity against HeLa (cervical cancer, CCL-2), COLO 205 (colon cancer, CCL-222), HepG2 (liver cancer, HB-8065), and MCF-7 (breast cancer, HTB-22) cell lines. Furthermore, the most active compounds were subjected to molecular docking studies to investigate their binding interactions with the selected biological target and to provide insights into their potential mechanism of action.

EXPERIMENTAL

^{1}H NMR spectra were recorded on Bruker AV 300 MHz in $CDCl_3$ & DMSO-d_6 using TMS as internal standard. ESI spectra were recorded on Micro mass, Quattro LC using ESI+ software with capillary voltage 3.98 kV and ESI mode positive ion trap detector. All high-resolution spectra were recorded on QSTARXL hybrid MS/MS system (Applied Biosystems, USA) under electrospray ionisation. All the reactions were monitored by thin layer chromatography (TLC) on precoated silica gel 60 F_{254}, spots were visualised with UV light. Merck silica gel (60-120 mesh) was used for column chromatography.

Synthesis of 2-amino-5-(trifluoromethyl)benzamide (2): A mixture of 2-amino-6-(trifluoromethyl)benzonitrile (0.5 g, 2.6 mmol), sodium ethoxide (3.2 mmol) and ethanol was heated under reflux with continuous stirring for 4 h. The progress of the reaction was monitored by TLC. Upon completion, the reaction mixture was poured onto crushed ice, resulting in the formation of a white solid. The precipitated product was collected by filtration, washed with cold water and dried to afford 2-amino-5-(trifluoromethyl)benzamide (**2**). Dark yellow solid; yield: 88%; IR (KBr, ν_{max}, cm^{-1}): 3661, 3425 (-NH_2), 3325 (COOH), 1624 (CO); ^{1}H NMR ($CDCl_3$, 300 MHz, δ ppm): 6.39 (br, s, 2H, -NH_2), 7.12 (d, 1H, Ar-H), 7.41 (d, 1H, Ar-H), 7.49 (br, s, 2H, -NH_2), 7.82 (s, 1H, Ar-H); MS (ESI): *m/z* [$(M+H)^+$]: 205; Anal. calcd. (found) % for $C_8H_7F_3N_2O$: C, 47.07 (47.09); H, 3.46 (3.49); N, 13.72 (13.76).

Synthesis of 6-(trifluoromethyl)quinazolin-4(3*H*)-one (3): 2-Amino-5-(trifluoromethyl)benzamide (2) (1.9 mmol) was refluxed in formic acid for 12 h. The progress of the reaction was monitored by TLC. After completion of the reaction, the reaction mixture was cooled and neutralized with $NaHCO_3$ solution. The resulting solid was washed thoroughly with water, filtered and dried to afford 6-(trifluoromethyl)-quinazolin-4(3*H*)-one (**3**). Yellow solid; yield: 76%; IR (KBr, ν_{max}, cm^{-1}): 3315, (CONH), 1632 (CO); ^{1}H NMR ($CDCl_3$, 300 MHz, δ ppm): 7.18 (s, 1H, Ar-H), 7.39 (d, 1H, Ar-H), 7.48 (d, 1H, Ar-H), 8.21 (s, 1H, Ar-H), 10.91 (br, s, 1H, -NH); MS (ESI): *m/z* [$(M+H)^+$]: 215; Anal. calcd. (found) % for $C_9H_5F_3N_2O$: C, 50.48 (50.50); H, 2.35 (2.37); N, 13.08 (13.11).

Synthesis of 6-(trifluoromethyl)quinazolin-4-amine (4): Charged 6-(trifluoromethyl)quinazolin-4(3*H*)-one (**3**), (2.3 mmol) 2-chloroacetamide (2.7 mmol) and 20 mg of K_2CO_3 in 10-15 mL of DMF, reaction mixture was allowed to reflux for 10-12 h. After completion of the reaction, as confirmed by TLC, the reaction mixture was poured onto crushed ice, resulting in the formation of a solid precipitate. The obtained solid was collected by filtration, washed thoroughly with water followed by *n*-hexane and dried to afford 6-(trifluoromethyl)-quinazolin-4-amine (**4**). Yellow solid; Yield: 68%; ^{1}H NMR ($CDCl_3$, 300 MHz, δ ppm): 6.52-6.55 (br, s, 2H, -NH_2), 7.26 (s, 1H, Ar-H), 7.39 (d, 1H, Ar-H), 7.52 (d, 1H, Ar-H), 8.32 (s, 1H, Ar-H); MS (ESI): *m/z* [$(M+H)^+$]: 214; Anal. calcd. (found) % for $C_9H_6F_3N_3$: C 50.71 (50.73); H, 2.84 (2.86); N, 19.71 (19.74).

10-(Trifluoromethyl)-4*H*-pyrimido[1,2-*c*]quinazolin-4-one (5a): Compound 6-(trifluoromethyl)quinazolin-4-amine (**4**) (0.5 g, 2.3 mmol) and ethyl 2-methyl-3-oxobutanoate (0.5 g, 3.5 mmol,) were mixed in 10-15 mL of ethanol followed by the addition of catalytic amount of acetic acid and then reflux for about 4-6 h. The progress of the reaction was monitored by TLC. Upon completion of the reaction, the mixture was cooled to room temperature, resulting in the formation of a product filtered, washed thoroughly and finally dried to afford 2,3-dimethyl-10-(trifluoromethyl)-4*H*-pyrimido[1,2-*c*]quinazolin-4-one (**5a-f**) (**Scheme-I**). White solid; yield: 76%; m.p.: 184-186 ºC; ^{1}H NMR ($CDCl_3$, 300 MHz, δ ppm): 7.05 (d, *J* = 7.8 Hz, 1H, Ar-H), 7.29 (d, *J* = 7.4 Hz, 1H, Ar-H), 7.45 (s, 1H, Ar-H), 7.55 (d, *J* = 7.4 Hz, 1H, Ar-H), 7.85 (d, *J* = 7.8 Hz, 1H, Ar-H), 8.05 (s, 1H, Ar-H); ^{13}C NMR ($CDCl_3$ 75 MHz, δ ppm): 120.8, 121.7, 122.4, 123.5, 124.6, 125.4, 127.3, 128.2, 129.2, 131.5, 134.7, 142.5, 143.6, 151.2, 152.2, 161.2; MS (ESI): *m/z* [$(M+H)^+$]: 266; Anal. calcd. (found) % for $C_{12}H_6F_3N_3O$: C, 54.35 (54.36); H, 2.28 (2.29), N 15.85 (15.88).

2-Methyl-10-(trifluoromethyl)-4*H*-pyrimido[1,2-*c*]-quinazolin-4-one (5b): Grey solid; yield: 70%; m.p.: 171-173 ºC; ^{1}H NMR ($CDCl_3$, 300 MHz, δ ppm): 2.28 (s, 3H, -CH_3), 7.06 (s, 1H, Ar-H), 7.29 (d, *J* = 7.8 Hz, 1H, Ar-H), 7.48 (d, *J* = 7.8 Hz, 1H, Ar-H), 7.82 (s, 1H, Ar-H) 8.02 (s, 1H, Ar-H); ^{13}C NMR ($CDCl_3$, 75 MHz, δ ppm): δ 23.3, 119.4, 120.7, 122.5, 123.4, 124.8, 125.7, 128.3, 130.5, 143.6, 150.4, 152.4, 161.5; MS (ESI): *m/z* [$(M+H)^+$]: 280; Anal. calcd. (found) % for $C_{13}H_8F_3N_3O$: C, 55.92 (55.94), H, 2.89 (2.88), N, 15.05 (15.09).

3-Ethyl-2-methyl-10-(trifluoromethyl)-4*H*-pyrimido-[1,2-*c*]quinazolin-4-one (5c): White solid; yield: 75%; m.p.: 195-197 ºC; ^{1}H NMR ($CDCl_3$, 300 MHz, δ ppm): 1.07 (t, 3H, -CH_3), 2.39 (q, 2H, -CH_2-), 2.75 (s, 3H, -CH_3), 7.31 (d, *J* = 7.8 Hz, 1H, Ar-H), 7.52 (d, *J* = 7.8 Hz, 1H, Ar-H), 7.79 (s, 1H, Ar-H) 8.05 (s, 1H, Ar-H); ^{13}C NMR ($CDCl_3$, 75 MHz, δ

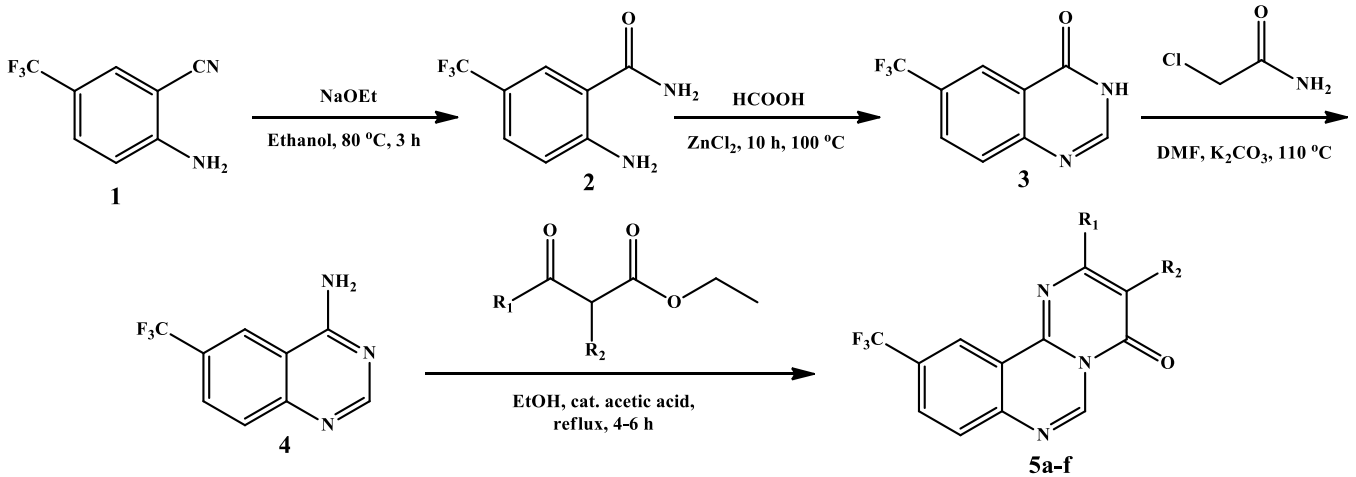

Scheme-I

ppm): 14.2, 19.5, 23.2, 120.5, 121.6, 123.6, 124.5, 126.3, 127.2, 128.4, 130.6, 142.5, 150.2, 152.6, 161.6; MS (ESI): *m/z* [(M+H)$^+$]: 308; Anal. calcd. (found) % for $C_{15}H_{12}F_3N_3O$: C, 58.63 (58.65); H, 3.94 (3.96), N, 13.68 (13.70).

2,3-Dimethyl-10-(trifluoromethyl)-4*H*-pyrimido[1,2-*c*]-quinazolin-4-one (5d): Grey solid; yield: 78%; m.p.: 147-149 ºC; ^{1}H NMR ($CDCl_3$, 300 MHz, δ ppm): 2.43 (s, 3H, -CH_3), 2.83 (s, 3H, -CH_3), 7.32 (d, *J* = 7.7 Hz, 1H, Ar-H), 7.48 (d, *J* = 7.7 Hz, 1H, Ar-H), 7.59 (s, 1H, Ar-H), 7.91 (s, 1H, Ar-H); ^{13}C NMR ($CDCl_3$, 75 MHz, δ ppm): 14.2, 22.9, 119.4, 120.7, 122.5, 123.5, 124.7, 125.6, 128.2, 132.6, 143.8, 150.3, 152.5, 161.6; MS (ESI): *m/z* [(M+H)$^+$]: 294; Anal. calcd. (found) % for $C_{14}H_{10}F_3N_3O$: C, 57.34 (57.36); H, 3.44 (3.46); N, 14.33 (14.36).

3-Ethyl-10-(trifluoromethyl)-4*H*-pyrimido[1,2-*c*]quinazolin-4-one (5e): White solid; yield: 75%; m.p.: 178-180 ºC; ^{1}H NMR ($CDCl_3$, 300 MHz, δ ppm): 1.09 (t, 3H, -CH_3), 2.35 (q, 2H, -CH_2-), 7.32 (d, *J* = 7.8 Hz, 1H, Ar-H), 7.43 (d, *J* = 7.8 Hz, 1H, Ar-H), 7.63 (s, 1H, Ar-H), 7.70 (s, 1H, Ar-H), 8.04 (s, 1H, Ar-H); ^{13}C NMR ($CDCl_3$, 75 MHz, δ ppm): 14.1, 20.5, 120.1, 121.5, 123.4, 125.7, 126.4, 127.1, 128.5, 130.4, 142.6, 150.1, 152.8, 161.8; MS (ESI): *m/z* [(M+H)$^+$]: 294; Anal. calcd. (found) % for $C_{14}H_{10}F_3N_3O$: C, 57.34 (57.31); H, 3.44 (3.45); N, 14.33 (14.35).

3-Methyl-10-(trifluoromethyl)-4*H*-pyrimido[1,2-*c*]-quinazolin-4-one (5f): White solid; yield: 64%; m.p.: 160-162 ºC; ^{1}H NMR ($CDCl_3$, 300 MHz, δ ppm): 2.46 (s, 3H, -CH_3), 7.11 (s, 1H, Ar-H), 7.31 (d, *J* = 7.8 Hz, 1H, Ar-H), 7.45 (d, *J* = 7.8 Hz, 1H, Ar-H), 7.71 (s, 1H, Ar-H) 8.00 (s, 1H, Ar-H); ^{13}C NMR ($CDCl_3$, 75 MHz, δ ppm): 14.5, 120.3, 121.6, 122.4, 123.6, 124.7, 126.5, 128.7, 130.6, 143.5, 150.2, 152.7, 161.6; MS (ESI): *m/z* [(M+H)$^+$]: 280; Anal. calcd. (found) % for $C_{13}H_8F_3N_3O$: C, 55.92 (55.90); H, 2.89 (2.87); N, 15.05 (15.07).

Synthesis of 4-chloro-6-(trifluoromethyl)quinazoline (6): Charged compound 6-(trifluoromethyl)quinazolin-4(3*H*)-one (**3**) (0.5 g, 2.3 mmol), 6-8 mL of $POCl_3$, the reaction mixture was allowed to reflux for 6 h. After completion of the reaction, as confirmed by TLC, excess $POCl_3$ was removed under reduced pressure. The resulting reaction mixture was then poured onto crushed ice, leading to the formation of a solid precipitate, collected, filtered, washed thoroughly with water followed by *n*-hexane and finally dried to afford 4-chloro-6-(trifluoromethyl)quinazoline (**6**). Yellow solid; yield: 75%; ^{1}H NMR ($CDCl_3$, 300 MHz, δ ppm): 7.26 (s, 1H, Ar-H), 7.39 (d, 1H, Ar-H), 7.52 (d, 1H, Ar-H), 8.32 (s, 1H, Ar-H); MS (ESI): *m/z* [(M+H)$^+$]: 233; Anal. calcd. (found) % for $C_9H_4ClF_3N_2$: C, 46.48 (46.50); H, 1.73 (1.75); N, 12.04 (12.06).

Synthesis of 4-hydrazinyl-6-(trifluoromethyl)quinazoline (7): A mixture of 4-chloro-6-(trifluoromethyl)quinazoline (**6**) (2.1 mmol) and hydrazine hydrate (10-15 mL) in ethanol was heated under reflux for 8-10 h. The progress of the reaction was monitored by TLC. Upon completion of the reaction, the mixture was poured onto crushed ice, resulting in the formation of a solid precipitate. The obtained solid was collected by filtration, washed thoroughly with water followed by *n*-hexane and dried to afford 4-hydrazinyl-6-(trifluoromethyl)quinazoline (**7**). Yellow solid; yield: 80%; ^{1}H NMR ($CDCl_3$, 300 MHz, δ ppm): 2.81-2.85 (br, s, 2H, -NH_2), 6.40 (br, s, 1H, -NH-), 7.28 (s, 1H, Ar-H), 7.41 (d, 1H, Ar-H), 7.54 (d, 1H, Ar-H), 8.29 (s, 1H, Ar-H); MS (ESI): *m/z* [(M+H)$^+$]: 229; Anal. calcd. (found) % for $C_9H_7F_3N_4$: C, 47.37 (47.36); H, 3.09 (3.10); N, 24.55 (24.58).

Synthesis of 3-phenyl-9-(trifluoromethyl)-[1,2,4]triazolo-[4,3-*c*]quinazoline (8a): A mixture of 2-hydrazinyl-3-phenyl-5-(trifluoromethyl)quinazolin-4(3*H*)-one (**5**) (0.5 g, 2.1 mmol), benzoic acid (0.4 g, 3.2 mmol) and $POCl_3$ (10-15 mL) was heated at 120 ºC for 6 h. The progress of the reaction was monitored by TLC. Upon completion of the reaction, the mixture was allowed to cool to room temperature and excess $POCl_3$ was removed under reduced pressure. Water was then added to the residue, resulting in the formation of a yellow solid. The precipitated product was collected by filtration, washed with water, and dried to afford compound **8a** (**Scheme-II**). Light yellow solid; yield: 78%; m.p.: 150-152 ºC; ^{1}H NMR ($CDCl_3$ 300 MHz, δ ppm): 7.33-7.38 (m, 3H, Ar-H), 7.45-7.48 (m, 2H, Ar-H), 7.61 (d, 1H, Ar-H), 7.69 (d, 1H, Ar-H), 8.05 (s, 1H, Ar-H), 8.63 (s, 1H, Ar-H); ^{13}C NMR ($CDCl_3$, 75 MHz, δ ppm): 118.3, 120.4, 121.5, 122.6, 123.7, 124.8, 126.4, 127.6, 128.6, 131.8, 136.7, 143.3, 150.3, 154.1; MS (ESI): *m/z* [(M+H)$^+$]: 315; Anal. calcd. (found) % for $C_{16}H_9F_3N_4$: C, 61.15 (61.16); H, 2.89 (2.87); N, 17.83 (17.85).

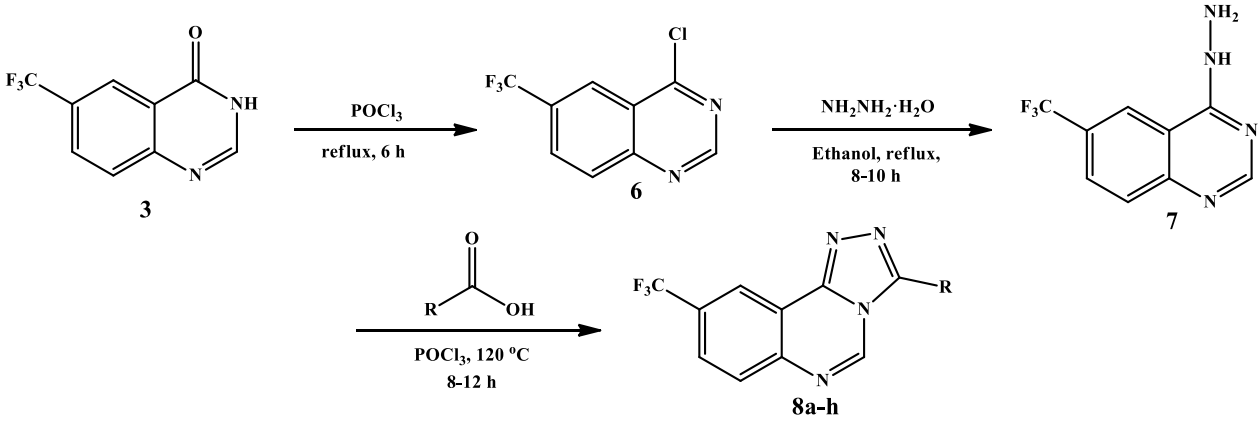

Scheme-II

3-(*p*-Tolyl)-9-(trifluoromethyl)-[1,2,4]triazolo[4,3-*c*]-quinazoline (8b): Light yellow solid; yield: 70%; m.p.: 163-165 ºC; ^{1}H NMR ($CDCl_3$, 300 MHz, δ ppm): 2.36 (s, 3H, Ar-CH_3), 7.29 (d, *J* = 7.8 Hz, 2H, Ar-H), 7.41 (d, *J* = 7.8 Hz, 2H, Ar-H), 7.59 (d, 1H, Ar-H), 7.67 (d, 1H, Ar-H), 8.01 (s, 1H, Ar-H), 8.51 (s, 1H, Ar-H); ^{13}C NMR ($CDCl_3$, 75 MHz, δ ppm): δ 21.6, 119.6, 120.5, 121.2, 122.7, 123.4, 124.5, 125.6, 127.4, 128.5, 132.7, 136.8, 142.6, 150.2, 153.3; MS (ESI): *m/z* [(M+H)$^+$]: 329; Anal. calcd. (found) % for $C_{17}H_{11}F_3N_4$: C, 62.20 (62.25); H, 3.38 (3.40); N, 17.07 (17.10).

3-(3-Methoxyphenyl)-9-(trifluoromethyl)-[1,2,4]triazolo[4,3-*c*]quinazoline (8c): Light yellow solid; yield: 70%; m.p.: 163-165 ºC; ^{1}H NMR ($CDCl_3$, 300 MHz, δ ppm): δ 3.82 (s, 3H, Ar-OCH_3), 7.32-7.36 (m, 3H, Ar-H), 7.47 (s, 1H, Ar-H), 7.55 (d, 1H, Ar-H), 7.64 (d, 1H, Ar-H), 7.95 (s, 1H, Ar-H), 8.33 (s, 1H, Ar-H); ^{13}C NMR ($CDCl_3$, 75 MHz, δ ppm): 55.6, 118.5, 120.4, 121.3, 122.6, 123.6, 124.4, 125.7, 126.5, 128.8, 132.4, 136.5, 138.5, 140.3, 142.7, 150.3, 153.4; MS (ESI): *m/z* [(M+H)$^+$]: 345; Anal. calcd. (found) % for $C_{17}H_{11}F_3N_4O$: C, 59.31 (59.32); H, 3.22 (3.25); N, 16.27 (16.30).

3-(3-Chlorophenyl)-9-(trifluoromethyl)-[1,2,4]triazolo-[4,3-*c*]quinazoline (8d): Yellow solid; yield: 78%; m.p.: 180-182 ºC; ^{1}H NMR ($CDCl_3$, 300 MHz, δ ppm): 7.30-7.33 (m, 3H, Ar-H), 7.49 (s, 1H, Ar-H), 7.56 (d, 1H, Ar-H), 7.65 (d, 1H, Ar-H), 7.98 (s, 1H, Ar-H), 8.25 (s, 1H, Ar-H); ^{13}C NMR ($CDCl_3$, 75 MHz, δ ppm): 118.4, 120.6, 121.3, 122.6, 123.5, 124.7, 125.8, 126.7, 127.4, 128.7, 130.5, 132.6, 136.7, 142.5, 150.7, 153.2; MS (ESI): *m/z* [(M+H)$^+$]: 349; Anal. calcd. (found) % for $C_{16}H_8ClF_3N_4$: C, 55.11 (55.13); H, 2.31 (2.34); N, 16.07 (16.09).

3-(3-Bromophenyl)-9-(trifluoromethyl)-[1,2,4]triazolo-[4,3-*c*]quinazoline (8e): Dark yellow solid; yield: 68%; m.p.: 169-170 ºC; ^{1}H NMR ($CDCl_3$, 300 MHz, δ ppm): 7.28-7.32 (m, 3H, Ar-H), 7.52 (s, 1H, Ar-H), 7.62 (d, 1H, Ar-H), 7.69 (d, 1H, Ar-H), 7.91 (s, 1H, Ar-H), 8.15 (s, 1H, Ar-H); ^{13}C NMR ($CDCl_3$, 75 MHz, δ ppm): 119.2, 120.3, 121.5, 122.6, 123.8, 124.4, 125.6, 126.8, 127.8, 128.5, 130.2, 132.7, 135.3, 142.3, 150.4, 153.6; MS (ESI): *m/z* [(M+H)$^+$]: 393; Anal. calcd. (found) % for $C_{16}H_8BrF_3N_4$: C, 48.88 (48.89); H, 2.05 (2.07); N, 14.25 (14.27).

3-(3-Fluorophenyl)-9-(trifluoromethyl)-[1,2,4]triazolo-[4,3-*c*]quinazoline (8f): Light cream solid; yield: 66%; m.p.: 152-154 ºC; ^{1}H NMR ($CDCl_3$, 300 MHz, δ ppm): δ 7.33-7.36 (m, 3H, Ar-H), 7.49 (s, 1H, Ar-H), 7.60 (d, 1H, Ar-H), 7.71 (d, 1H, Ar-H), 7.95 (s, 1H, Ar-H), 8.18 (s, 1H, Ar-H); ^{13}C NMR ($CDCl_3$, 75 MHz, δ ppm): 118.5, 120.4, 121.6, 122.5, 123.7, 124.6, 125.7, 126.4, 127.4, 129.6, 131.3, 132.5, 135.6, 142.4, 150.4, 152.5; MS (ESI): *m/z* [(M+H)$^+$]: 333; Anal. calcd. (found) % for $C_{16}H_8F_4N_4$: C, 57.84 (57.86); H, 2.43 (2.45); N, 16.86 (16.88).

9-(Trifluoromethyl)-3-(3-(trifluoromethyl)phenyl)-[1,2,4]triazolo[4,3-*c*]quinazoline (8g): Yellow green solid; yield: 66%; m.p.: 188-189 ºC; ^{1}H NMR ($CDCl_3$, 300 MHz, δ ppm): 7.35-7.38 (m, 3H, Ar-H), 7.48 (s, 1H, Ar-H), 7.61 (d, 1H, Ar-H), 7.78 (d, 1H, Ar-H), 7.91 (s, 1H, Ar-H), 8.24 (s, 1H, Ar-H); ^{13}C NMR ($CDCl_3$, 75 MHz, δ ppm): 118.8, 120.4, 121.5, 122.3, 123.6, 124.5, 125.8, 126.5, 127.8, 129.8, 131.2, 132.6, 135.8, 142.4, 143.9, 150.4, 152.5; MS (ESI): *m/z* [(M+H)$^+$]: 383; Anal. calcd. (found) % for $C_{17}H_8F_6N_4$: C, 53.41 (53.43); H, 2.11 (2.13); N, 14.66 (14.68).

4-(9-(Trifluoromethyl)-[1,2,4]triazolo[4,3-*c*]quinazolin-3-yl)phenol (8h): Grey solid; yield: 66%; m.p.: 196-198 ºC; ^{1}H NMR ($CDCl_3$, 300 MHz, δ ppm): 5.27 (br, s, 1H, Ar-OH), 7.27 (d, *J* = 7.7 Hz, 2H, Ar-H), 7.39 (d, *J* = 7.7 Hz, 2H, Ar-H), 7.55 (d, 1H, Ar-H), 7.67 (d, 1H, Ar-H), 7.97 (s, 1H, Ar-H), 8.25 (s, 1H, Ar-H); ^{13}C NMR ($CDCl_3$, 75 MHz, δ ppm): 120.1, 121.4, 122.6, 123.5, 124.8, 125.7, 127.3, 128.6, 132.8, 136.9, 142.5, 150.4, 153.4, 156.8; MS (ESI): *m/z* [(M+H)$^+$]: 331; Anal. calcd. (found) % for $C_{16}H_9F_3N_4O$: C, 58.19 (58.20); H, 2.75 (2.78); N, 16.96 (16.98).

Molecular docking studies: Molecular docking studies were carried out using AutoDock 4.2 to evaluate the binding interactions of the synthesised compounds with the target protein (PDB ID: 4HJO), retrieved from the Protein Data Bank. Prior to docking, co-crystallized ligands and water molecules were removed, followed by the addition of polar hydrogen atoms and assignment of Gasteiger charges. The ligand structures were drawn using ChemDraw 12.0, energy-minimized, and converted from MOL to PDB format using Discovery Studio. A grid box of 42 Å × 44 Å × 42 Å was defined around the active site and docking simulations were performed using the Lamarckian Genetic Algorithm implemented in AutoDock 4.2. The docking runs were executed through the Cygwin interface and the generated docking log files were analyzed

to obtain the binding conformations and docking scores. The docked complexes were visualized using Maestro Visualizer (Schrödinger Suite v9.5), and the protein–ligand interactions were examined through two-dimensional and three-dimensional representations.

Cytotoxicity activity: The cytotoxic activity of the synthesised compounds was evaluated by measuring *in vitro* growth inhibitory effects on human cancer cell lines using the MTT assay in 96-well plates [39]. The assay is based on the reduction of tetrazolium salt to water-insoluble formazan crystals by viable cells. 5-Fluorouracil was employed as the reference standard. Cytotoxicity was assessed against four human cancer cell lines *viz*. HeLa (human cervical cancer, ATCC CCL-2), COLO 205 (human colon cancer, ATCC CCL-222), HepG2 (human liver cancer, ATCC HB-8065) and MCF-7 (human breast adenocarcinoma, ATCC HTB-22). The IC_{50} values (50% inhibitory concentration) were determined from the dose–response curves generated using absorbance measurements. The results are expressed as mean ± SD (μM) from three independent experiments.

RESULTS AND DISCUSSION

A series of novel pyrimido[1,2-*c*]quinazolin-4-one and triazolo[4,3-*c*]quinazoline derivatives were synthesised starting from 2-amino-5-(trifluoromethyl)benzonitrile (**1**). Basic hydrolysis of compound **1** using NaOH in aqueous ethanol afforded 2-amino-5-(trifluoromethyl)benzamide (**2**), which upon cyclisation with formic acid in the presence of $ZnCl_2$ yielded 6-(trifluoromethyl)quinazolin-4(3*H*)-one (**3**). Subsequent reaction of compound **3** with 2-chloroacetamide in the presence of K_2CO_3 and NaI in DMF afforded 6-(trifluoromethyl)quinazolin-4-amine (**4**). Condensation of compound **4** with various substituted ethyl 2-methyl-3-oxobutanoates in refluxing ethanol containing catalytic acetic acid furnished the target pyrimido-[1,2-*c*]quinazolin-4-one derivatives (**5a-f**). In a parallel synthetic route, compound 3 was treated with $POCl_3$ under reflux to obtain 4-chloro-6-(trifluoromethyl)quinazoline (**6**). Nucleophilic substitution of compound **6** with hydrazine hydrate in refluxing ethanol afforded 4-hydrazinyl-6-(trifluoromethyl)-quinazoline (**7**). Finally, cyclocondensation of compound **7** with various aromatic acids in the presence of $POCl_3$ at 120 ºC yielded the corresponding triazolo[4,3-*c*]quinazoline derivatives (**8a-h**).

Molecular docking studies: To gain insight into the possible binding mode of the most active compounds, molecular docking studies were performed using the AutoDock protocol implemented in PyRx 0.8. The synthesised compounds **5a** and **5c**, along with the reference drug 5-fluorouracil, were docked into the active site of the human epidermal growth factor receptor (EGFR) tyrosine kinase domain (PDB ID: 4HJO) [39,40]. The docking results, including binding energies, hydrogen-bonding interactions and key amino acid residues involved in ligand recognition, are summarized in Table-1.

Compound **5a** exhibited a binding energy of -5.90 kcal mol^{-1} and formed a hydrogen bond with LYS721 through the quinazoline nitrogen atom acting as a hydrogen-bond acceptor. Additional stabilization within the binding pocket was provided by interactions with ALA719, VAL702, THR766 and LEU820 through carbon–hydrogen bonds, π-sigma interactions, alkyl contacts and π-alkyl interactions. The interaction profile suggests that compound **5a** is favourably accommodated within the ATP-binding region of EGFR through a combination of polar and hydrophobic interactions (Fig. 1). Among the investigated compounds, derivative **5c** displayed the highest binding affinity with a docking score of -6.49 kcal mol^{-1}. Compound **5c** established three hydrogen bonds with THR766, MET769 and CYS773 involving the carbonyl oxygen, quinazoline nitrogen and fluorine atom of the trifluoromethyl substituent, respectively. In addition, interactions with GLN767, LEU694, LEU820, ALA719 and LYS721, including hydrogen-bonding, halogen-bonding, π-sigma and hydrophobic interactions, further contributed to the stabilization of the ligand within the active site. The extensive interaction network and favourable orientation of **5c** within the binding cavity (Fig. 2) are consistent with its superior docking score relative to compound **5a** and the reference drug. In comparison, 5-fluorouracil exhibited a lower binding affinity of -3.94 kcal mol^{-1} despite forming four hydrogen bonds. Key interactions involved residues LYS721, ASP831 and THR830 through the carbonyl oxygen and amide functionalities of the ligand. Despite forming multiple hydrogen bonds, the lack of significant hydrophobic and π-mediated interactions may compromise binding stability within the active site, contributing to its lower docking score (Fig. 3).

Visualization of the protein-ligand complexes (Fig. 4) further highlighted the distinct binding behaviour of the evaluated ligands. Compound **5c** occupied the active site more effectively than compound **5a** and 5-fluorouracil, establishing multiple favourable interactions that collectively enhanced binding affinity. These observations emphasize the importance of the quinazoline framework and the trifluoromethyl substituent in promoting productive interactions within the EGFR binding pocket. The docking results showed good agreement

TABLE-1
MOLECULAR INTERACTION OF BIOLOGICALLY POTENT HYBRIDS (**5a, 5c** AND 5-FLUOROURACIL**)** WITH HUMAN EGFR TKD PROTEIN

Compounds	Binding energy (Kcal/mol)	Number of hydrogen bonds	Interacting amino acids	Nature of interactions
5a	-5.90	1	**LYS721**, ALA719, VAL702, THR766, LEU820	H-bond, Carbon hydrogen bond, Pi-Sigma, Alkyl, Pi-Alkyl
5c	-6.49	3	**THR766**, **MET769**, **CYS773**, GLN767, LEU694, LEU820, ALA719, LYS721	H-bond, Carbon hydrogen bond, Halogen (fluorine) Pi-Sigma, Alkyl, Pi-Alkyl
5-Fluorouracil	-3.94	4	**LYS721**, **THR830**, **ASP831**, LEU834	H-bond, Pi-Anion, Pi-Alkyl

H-bond forming residues in bold.

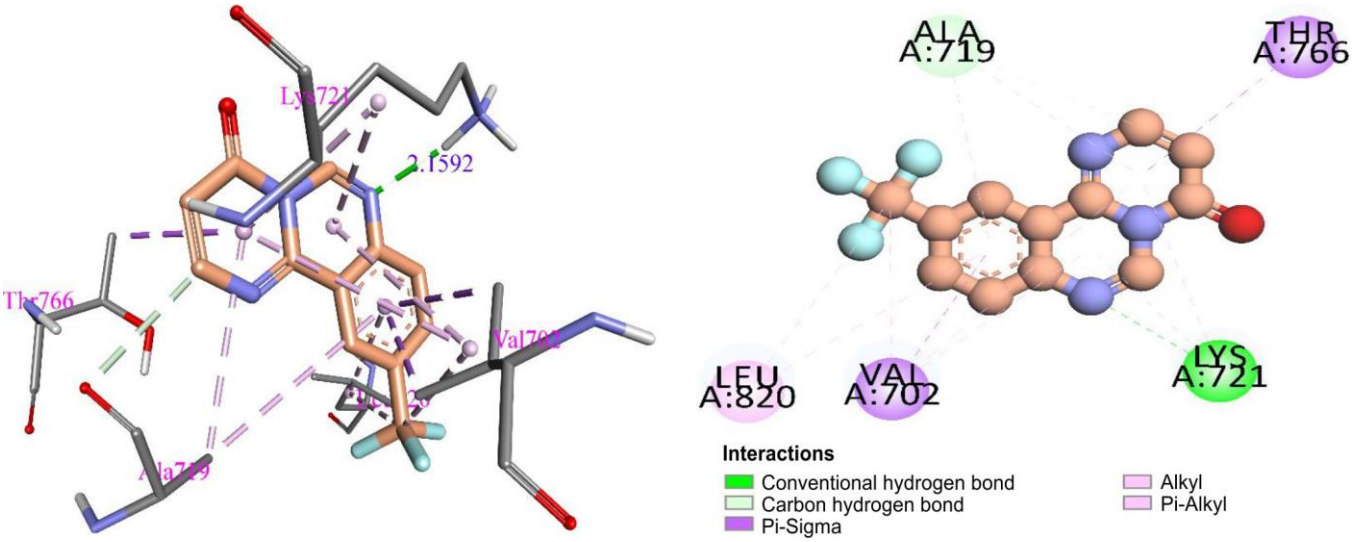

Fig. 1. 3D and 2D images of **5a** binding configurations docked into the EGFR active site

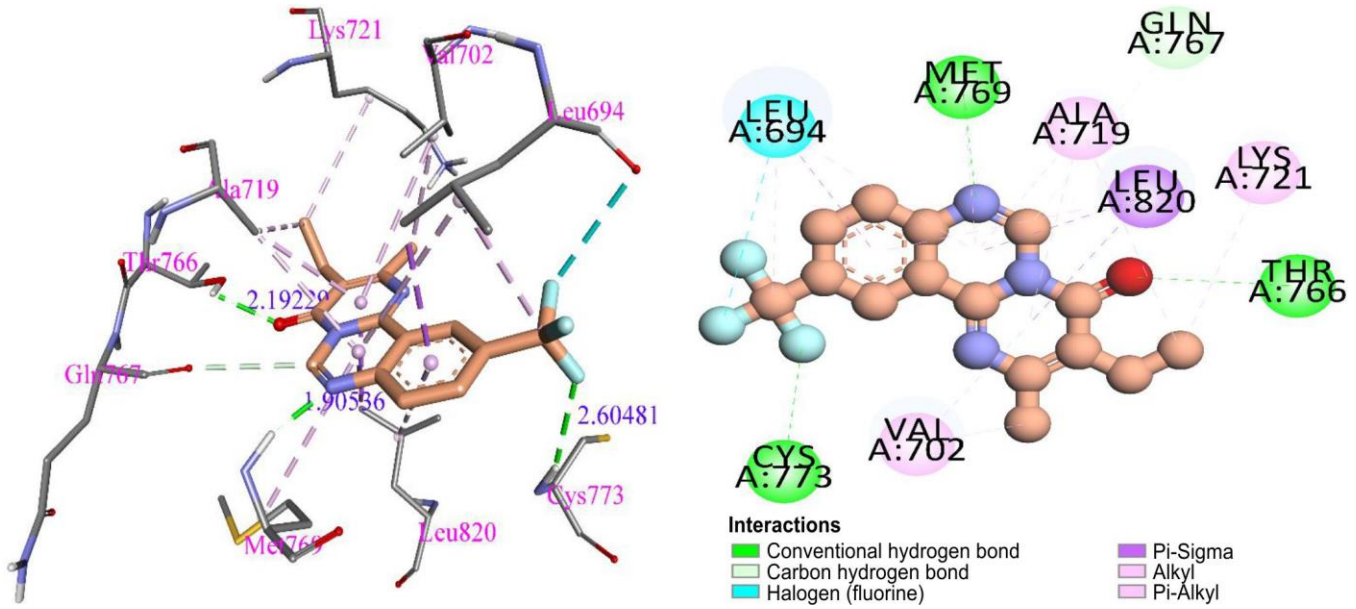

Fig. 2. 3D and 2D images of **5c** binding configurations docked into the EGFR active site

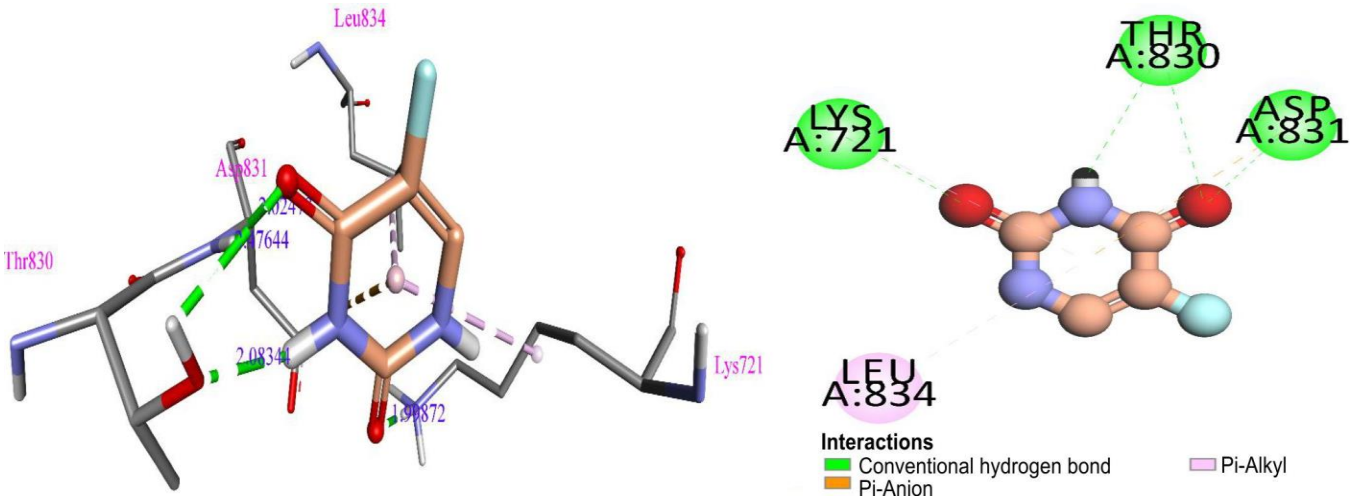

Fig. 3. 3D and 2D images of 5-fluorouracil binding configurations docked into the EGFR active site

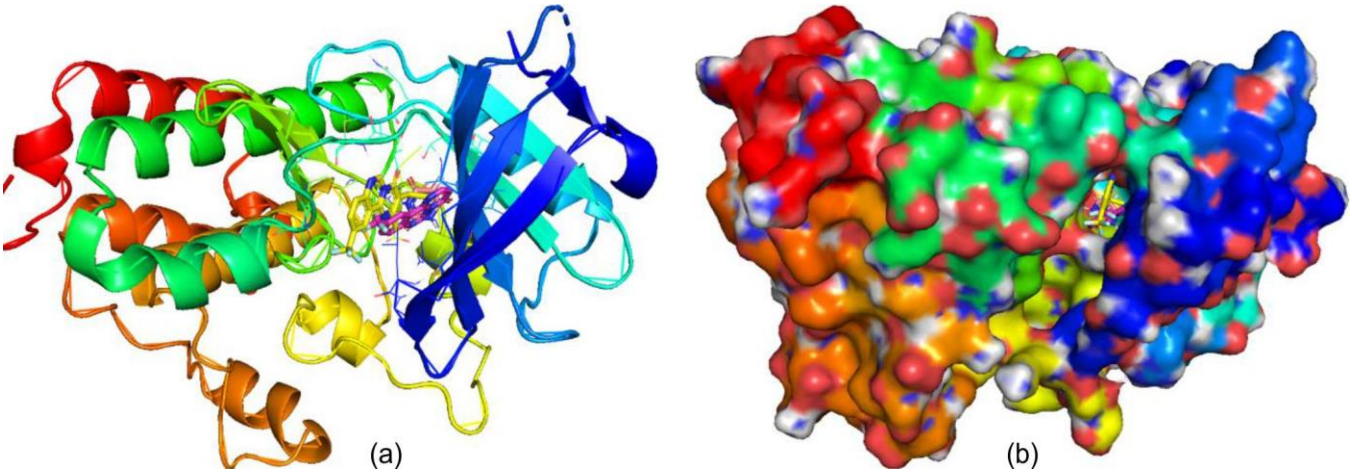

Fig. 4. (a) Protein-ligands complex of **5a** (pink colour), **5c** (yellow colour) and 5-fluorouracil (gold colour) within the active site of EGFR TKD; (b) protein surface representation of EGFR TKD the compounds **5a** (pink colour), **5c** (yellow colour) and 5-fluorouracil (gold colour) in the active site pocket

with the experimental anticancer activity, where compound **5c** emerged as the most active derivative. The enhanced activity of compounds bearing electron-withdrawing substituents, particularly the trifluoromethyl group, may be attributed to improved hydrophobic interactions and more favourable accommodation within the EGFR active site. Furthermore, the fused quinazoline scaffold provides a rigid molecular architecture capable of engaging in multiple stabilizing interactions with key amino acid residues located in the ATP-binding domain. The docking results correlate well with the experimental anticancer data, identifying compound **5c** as the most promising derivative. However, molecular docking studies provide only preliminary insights into protein-ligand interactions and are insufficient to establish EGFR inhibition as the primary mechanism responsible for the observed cytotoxic activity. Consequently, additional biological studies, including EGFR kinase inhibition and apoptosis assays, are required to confirm the proposed mode of action and further evaluate the therapeutic potential of these compounds.

Cytotoxicity activity: All the synthesized target compounds **5a-f** and **8a-h** were evaluated for their *in vitro* anticancer activity against four human cancer cell lines, namely HeLa (cervical cancer, CCL-2), COLO 205 (colon cancer, CCL-222), HepG2 (liver cancer, HB-8065) and MCF-7 (breast cancer, HTB-22) using the MTT assay [38]. 5-Fluorouracil was employed as the reference standard. The anticancer activity data expressed as IC_{50} values (μM) are presented in Table-2. Most of the synthesized compounds exhibited significant cytotoxic activity against the tested cell lines, whereas some derivatives did not show significant inhibition up to a concentration of 120.1 μM. Comparative analysis of the cytotoxicity data revealed that pyrimido[1,2-*c*]quinazolin-4-ones generally displayed superior anticancer activity relative to the triazolo-[4,3-*c*]quinazoline analogues. Among the tested compounds, derivatives **5a** and **5c** emerged as the most potent members of the series, exhibiting IC_{50} values in the range of 13.6-19.4 μM against the evaluated cancer cell lines.

TABLE-2
In vitro CYTOTOXICITY ACTIVITY DATA OF COMPOUNDS **5a-f** AND **8a-j**

Compounds	IC_{50} values (μM)			
	HeLa (cervical cancer)	COLO 205 (colon cancer)	HepG2 (liver cancer)	MCF-7 (breast cancer)
5a	18.2 ± 2.35	–	15.2 ± 3.51	–
5b	43.5 ± 2.51	39.6 ± 1.25	25.2 ± 3.23	46.2 ± 2.18
5c	13.6 ± 1.12	19.4 ± 0.34	15.5 ± 1.25	–
5d	45.2 ± 3.26	29.6 ± 3.25	26.2 ± 2.25	–
5e	53.5 ± 0.23	71.5 ± 3.24	–	84.6 ± 2.18
5f	–	–	–	–
8a	48.5 ± 1.16	54.6 ± 0.31	24.5 ± 2.54	40.6 ± 2.13
8b	–	31.5 ± 1.65	55.8 ± 2.25	–
8c	14.9 ± 4.18	–	–	120.1 ± 3.25
8d	–	–	–	–
8e	–	–	59.1 ± 2.25	–
8f	–	–	–	–
8g	–	–	–	–
8h	–	–	–	–
5-Fluorouracil (std. control)	1.8 ± 0.09	1.9 ± 0.11	1.7 ± 0.08	1.8 ± 0.07

– indicates IC_{50} value >120.1 μM

Conclusion

In conclusion, a series of novel pyrimido[1,2-*c*]quinazolin-4-one (**5a-f**) and triazolo[4,3-*c*]quinazoline (**8a-h**) derivatives were successfully designed and synthesized. The structures of the synthesized compounds were established through IR, ^{1}H NMR, ^{13}C NMR and ESI-MS spectral analyses. The synthesised derivatives were evaluated for their *in vitro* anticancer activity against four human cancer cell lines, namely HeLa (cervical cancer), COLO 205 (colon cancer), HepG2 (liver cancer) and MCF-7 (breast cancer), using the MTT assay. Among the studied compounds, derivatives **5a** and **5c** exhibited the most promising anticancer activity. Molecular docking studies further supported their potential interactions within the EGFR active site, with compound **5c** displaying the most favourable binding profile. Although the docking results provide preliminary insight into the possible mode of action of these compounds, the proposed EGFR inhibitory potential requires further validation through detailed biochemical, enzymatic, and mechanistic investigations. These findings highlight the potential of quinazoline-based fused heterocyclic systems as promising scaffolds for the development of new anticancer agents.

CONFLICT OF INTEREST

The authors declare that there is no conflict of interests regarding the publication of this article.

DECLARATION OF AI-ASSISTED TECHNOLOGIES

During the preparation of this manuscript, the authors used an AI-assisted tool(s) to improve the language. The authors reviewed and edited the content and take full responsibility for the published work.

REFERENCES

1. P. Anastas and N. Eghbali, *Chem. Soc. Rev.*, **39**, 301 (2010); https://doi.org/10.1039/B918763B
2. T.E. Nielsen and S.L. Schreiber, *Angew. Chem. Int. Ed.*, **47**, 48 (2008); https://doi.org/10.1002/anie.200703073
3. A.A. Kadi, N.R. El-Brollosy, O.A. Al-Deeb, E.E. Habib, T.M. Ibrahim and A.A. El-Emam, *Eur. J. Med. Chem.*, **42**, 235 (2007); https://doi.org/10.1016/j.ejmech.2006.10.003
4. M.M. Ghorab, Z.H. Ismail, A.A. Radwan and M. Abdalla, *Acta Pharm.*, **63**, 1 (2013); https://doi.org/10.2478/acph-2013-0006
5. N. Kushwaha, A. Sahu, J. Mishra, A. Soni and D. Dorwal, *Curr. Org. Synth.*, **20**, 838 (2023); https://doi.org/10.2174/1570179420666230316094435
6. A.S. El-Azab and K.E. El-Tahir, *Bioorg. Med. Chem. Lett.*, **22**, 1879 (2012); https://doi.org/10.1016/j.bmcl.2012.01.071
7. A.A. Radwan, F.K. Alanazi and A. Al-Dhfyan, *Drug Res.*, **63**, 129 (2013); https://doi.org/10.1055/s-0032-1333306
8. S.R. Pathak, V. Malhotra, R. Nath and K. Shanker, *Cent. Nerv. Syst. Agents Med. Chem.*, **14**, 34 (2014); https://doi.org/10.2174/18715249146661408251447 29
9. M.S. Malamas and J. Millen, *J. Med. Chem.*, **34**, 1492 (1991); https://doi.org/10.1021/jm00108a038
10. K.P. Rakesh, H.M. Manukumar and D.C. Gowda, *Bioorg. Med. Chem. Lett.*, **25**, 1072 (2015); https://doi.org/10.1016/j.bmcl.2015.01.010
11. B. Yousefi, A. Azimi, M. Majidinia, V. Shafiei-Irannejad, R. Badalzadeh, B. Baradaran, N. Zarghami and N. Samadi, *Tumour Biol.*, **39**, 1 (2017); https://doi.org/10.1177/1010428317716501
12. P. Traxler, J. Green, H. Mett, U. Séquin and P. Furet, *J. Med. Chem.*, **42**, 1018 (1999); https://doi.org/10.1021/jm980551o
13. M. Sahu and A.G. Nerkar, *Int. J. Pharm. Pharm. Sci.*, **6**, 193 (2014).
14. L. Ôrfi, J. Kökösi, G. Szász, I. Kövesdi, M. Mák, I. Teplán and G. Kéri, *Bioorg. Med. Chem.*, **4**, 547 (1996); https://doi.org/10.1016/0968-0896(96)00040-5
15. M.J. Hour, L.J. Huang, S.C. Kuo, Y. Xia, K. Bastow, Y. Nakanishi, E. Hamel and K.-H. Lee, *J. Med. Chem.*, **43**, 4479 (2000); https://doi.org/10.1021/jm000151c
16. R. Bouley, D. Ding, Z. Peng, M. Bastian, E. Lastochkin, W. Song, M.A. Suckow, V.A. Schroeder, W.R. Wolter, S. Mobashery and M. Chang, *J. Med. Chem.*, **59**, 5011 (2016); https://doi.org/10.1021/acs.jmedchem.6b00372
17. A.J. Bojarski, P. Kowalski, T. Kowalska, B. Duszyńska, A. Kłodzińska, E. Tatarczyńska, S. Charakchieva-Minol and E. Chojnacka-Wójcik, *Bioorg. Med. Chem.*, **10**, 3817 (2002); https://doi.org/10.1016/S0968-0896(02)00349-8
18. J.A. Grosso, D.E. Nichols, J.D. Kohli and D. Glock, *J. Med. Chem.*, **25**, 703 (1982); https://doi.org/10.1021/jm00348a018
19. Y.A. Mohamed, A.E.-G. Amr, S.F. Mohamed, M.M. Abdalla, M.A. Al-Omar and S.H. Shfik., *J. Chem. Sci.*, **124**, 693 (2012); https://doi.org/10.1007/s12039-012-0242-4
20. P. Sharma, N. Rane and V.K. Gurram, *Bioorg. Med. Chem. Lett.*, **14**, 4185 (2004); https://doi.org/10.1016/j.bmcl.2004.06.014
21. H.S. Basavaraja, G.M. Sreenivasa and E. Jayachandran, *Indian J. Heterocycl. Chem.*, **15**, 69 (2005).
22. M. Amir, S.A. Javed and H. Kumar, *Indian J. Pharm. Sci.*, **69**, 337 (2007); https://doi.org/10.4103/0250-474X.34540
23. S.M. Sondhi, S. Jain, A.D. Dwivedi, R. Shukla and R. Raghubir, *Indian J. Chem.*, **47B**, 136 (2008).
24. A.A. Abu-Hashem, M.M. Youssef and H.A.R. Hussein, *J. Chin. Chem. Soc.*, **58**, 41 (2011); https://doi.org/10.1002/jccs.201190056
25. K. Colanceska-Ragenovic, V. Dimova, V. Kakurinov, D.G. Molnar and A. Buzarovska, *Molecules*, **6**, 815 (2001); https://doi.org/10.3390/61000815
26. Z. Xu, S.-J. Zhao and Y. Liu, *Eur. J. Med. Chem.*, **183**, 111700 (2019); https://doi.org/10.1016/j.ejmech.2019.111700
27. S. Cai, Q.-S. Li, R.T. Borchardt, K. Kuczera and R.L. Schowen, *Bioorg. Med. Chem.*, **15**, 7281 (2007); https://doi.org/10.1016/j.bmc.2007.08.029
28. A.H. Groll and T.J. Walsh, *Swiss Med. Wkly.*, **132**, 303 (2002); https://doi.org/10.4414/smw.2002.09729
29. M.A. Ghannoum and L.B. Rice, *Clin. Microbiol. Rev.*, **12**, 501 (1999); https://doi.org/10.1128/CMR.12.4.501
30. A.U. Buzdar, J.F. Robertson, W. Eiermann and J.-M. Nabholtz, *Cancer*, **95**, 2006 (2002); https://doi.org/10.1002/cncr.10908
31. J. Geisler, H. Helle, D. Ekse, N.K. Duong, D.B. Evans, Y. Nordbø, T. Aas and P.E. Lønning, *Clin. Cancer Res.*, **14**, 6330 (2008); https://doi.org/10.1158/1078-0432.CCR-07-5221
32. S.G. Küçükgüzel and P. Çıkla-Süzgün, *Eur. J. Med. Chem.*, **97**, 830 (2015); https://doi.org/10.1016/j.ejmech.2014.11.033
33. I. Khan, S. Zaib, S. Batool, N. Abbas, Z. Ashraf, J. Iqbal and A. Saeed, *Bioorg. Med. Chem.*, **24**, 2361 (2016); https://doi.org/10.1016/j.bmc.2016.03.031
34. G.S. Kumar, Y. Poornachandra, S.K. Gunda, K.R. Reddy, J. Mohmed, K. Shaik, C.G. Kumar and B. Narsaiah, *Bioorg. Med. Chem. Lett.*, **28**, 2328 (2018); https://doi.org/10.1016/j.bmcl.2018.04.031
35. S. Betala, N. Puram and U. Bhanothu, *Lett. Org. Chem.*, **21**, 575 (2024); https://doi.org/10.2174/0115701786272432231211100408
36. J. Chae, T. Konno, T. Ishihara and H. Yamanaka, *Chem. Lett.*, **33**, 314 (2004); https://doi.org/10.1246/cl.2004.314
37. B. Udayasri, P. Naveen and B. Sailu, *Russ. J. Gen. Chem.*, **95**, 864 (2025); https://doi.org/10.1134/S1070363224612729
38. T. Mosmann, *J. Immunol. Methods*, **65**, 55 (1983); https://doi.org/10.1016/0022-1759(83)90303-4
39. S. Amudala, R. Palabindela, S. Bhoomandla, N. Kotilingaiah, J. Sandhya and J. Mandala, *Russ. J. Bioorg. Chem.*, **50**, 34 (2024); https://doi.org/10.1134/S1068162024010138
40. A. Ambala, J. Sandhya, N. Kotilingaiah, M. Sudha, S. Pandiri and R. Palabindela, *Biochem. Biophys. Res. Commun.*, **786**, 152723 (2025); https://doi.org/10.1016/j.bbrc.2025.152723